**3.5**

# THE IMPORTANCE OF INCLUDING ANTHROPOGENIC HEATING IN MESOSCALE MODELING OF THE URBAN HEAT ISLAND

David J. Sailor*
Portland State University, Portland, Oregon
and
Hongli Fan
Tulane University, New Orleans, Louisiana

## 1. INTRODUCTION

The surface characteristics and anthropogenic activities in the urban environment often lead to local warming relative to the rural surroundings – a phenomenon known as the Urban Heat Island (UHI). The UHI is typically largest during evening hours and during the winter. Nevertheless, the UHI effect in summer can be of particular interest with respect to its impact on urban air quality, air conditioning energy demand, human comfort, and heat-related illness. The urban-rural differences in albedo, moisture, roughness, and thermal capacitance are often cited as the key causes for the urban heat island. Studies that focus on the role that these parameters play in the development of the UHI are common (e.g., Carlson and Arthur, 2000; Hafner and Kidder, 1999; Owen et al., 1998; Taha et al., 1991). Anthropogenic heating is also a potential factor in the urban heat island, but is often dismissed under the assumption that it is relatively small in magnitude. While it is true that anthropogenic heating is small compared with summertime mid-day solar insolation, it plays a major role in the surface energy balance at times when the urban heat island effect is at its maximum (night time and winter). Recent studies suggest that anthropogenic heating, in fact, may be a significant contributor to the UHI (Fujino et al., 1996; Ichinose, 1999; Sailor, 2003). Additional studies are needed, however, to quantify the role of anthropogenic heating in the urban climate, and provide guidance with respect to the value of including it as a source term in modeling efforts. This serves as the motivation for the present work.

This paper will summarize the development and implementation of seasonal profiles of anthropogenic heating in mesoscale models of cities. Observations of the urban heat island will be compared with modeled urban warming associated with anthropogenic heating (in the absence of a detailed urban canopy parameterization). Conclusions will focus on the nominal fraction of the heat island that may be explained by anthropogenic heating as well as fundamental issues regarding the appropriate implementation of such heating in mesoscale models.

## 2. ANTHROPOGENIC HEAT ($Q_F$) PROFILES

To avoid the extreme cost of gathering detailed building-level data for estimating anthropogenic heating ($Q_f$) profiles we have developed a top-down approach that relies on easily obtained energy and population data at aggregate spatial and temporal scales. This methodology is described in detail by (Sailor, 2003). For the purposes of the present paper a quick background of the general methodology is provided below.

Per capita energy consumption data (electricity and heating fuels) are obtained from the Energy Information Administration (EIA) of the U.S. Department of Energy. These data are mapped onto diurnal profiles using generalized profile functions that are based on data from across the United States.

In many urban areas the population density in the urban core increase substantially during the workday due to commuting workers and others who visit the city during the day. So, simply using resident population data from US Census records is not sufficient. We estimate diurnal profiles of urban population density based on the "journey to work" data base from the US census' Urban Transportation Planning Package (UTPP). The general approach is similar to that suggested by (Fulton, 1984). Specifically,

$$\rho_{pop\_day} = \frac{NWRP + WP}{A} \qquad (1)$$

where NWRP is the non-working resident population (from traditional census records), WP is the working population in the urban area (from UTPP data), and A is the extent of the urban area or relevant census tract. The hourly population density is obtained by merging the daytime and nighttime (resident) population densities with a suitable transition period in the morning and evening. At the present time we have defined diurnal population density profiles at the city scale, although extending this analysis down to the census

* Corresponding author address: David J. Sailor, Portland State Univ., PO 751, Portland, OR 97207; email: sailor@cecs.pdx.edu

tract scale is feasible, and desirable in certain applications.

### 2.2. Vehicular emissions

Heat released from vehicles is estimated by obtaining daily vehicle miles traveled (DVMT) data from the US Department of Transportation for the city of interest. The per capita DVMT is then mapped onto a diurnal profile using a standardized profile for fractional daily traffic within each hour. This standardized profile is based on detailed data from multiple sources (Dreher and Harley, 1998; Gammariello and Carlock, 1997; Hallenbeck et al., 1997; ISTHA, 1998; Larsen, 2000). The corresponding fractional traffic profiles are given in Figure 1, and show striking similarities, with comparable size peaks for both the morning and evening rush hours. Given the similarity among such profiles, we simply use the average of these profiles (bold line in Figure 1) in developing vehicular emissions profiles.

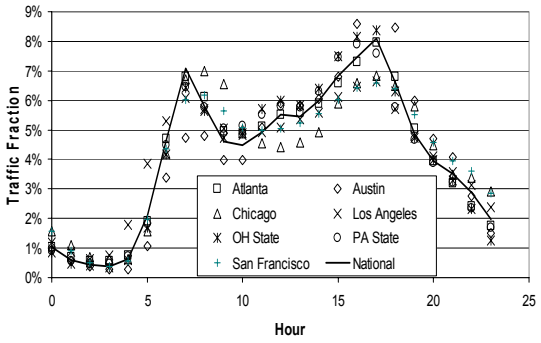


**Figure 1**. Hourly fraction profiles for vehicular traffic in the United States.

### 2.3. Building sector

Waste heat generated by hourly energy consumption is rejected from buildings into the surrounding environment through air conditioning and ventilation systems, through building leakage (air exchanges), and via heat transfer through building walls. The challenge is to obtain the necessary energy consumption data at both the required spatial resolution (city-scale or finer) and the required temporal resolution (hourly). The U.S. Department of Energy collects monthly totals of consumption of electricity and other fuels aggregated at the state level. These data are available through the Energy Information Administration (EIA, Electric Power Monthly and related publications).

To map per capita monthly electricity consumption onto hourly profiles we can access load profile functions from electric utilities and associated regional Independent Service Operators (ISO) across the country. These profile functions have surprising similarities as illustrated in Figure 2. So, even though the daily per capita consumption ($E_{DPC}$) differs regionally, the generalized diurnal profile functions may be applied to commonly available aggregate data to obtain hourly consumption profiles:

$$E_{BE} = E_{\mathrm{DPC}} \cdot f(hour) \text{, where } \sum_{1}^{24} f(hour) = 1.0 \qquad (3)$$

As with electricity consumption, the EIA collects and archives state monthly usage totals for various combustion fuels (natural gas, LPG, kerosene, fuel oil). Our analysis maps monthly state aggregate values of per capita heating fuel consumption to a diurnal profile using established relationships between fuel consumption and ambient temperature (Sailor, 1998) and representative diurnal temperature profiles for the cities of interest.

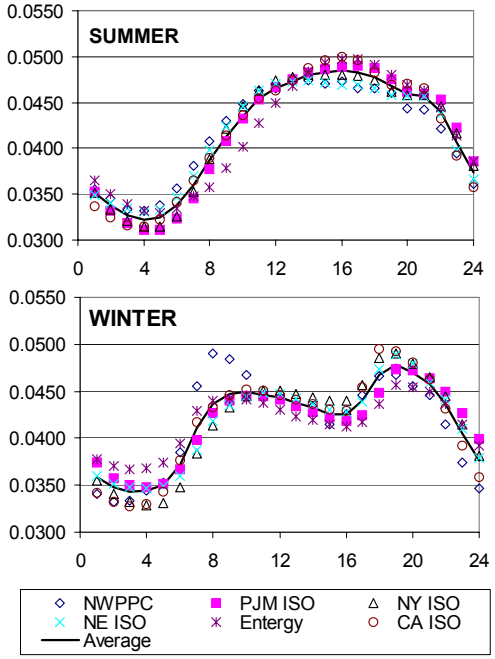


**Figure 2**. Electricity load profiles (hourly fractions) for different service operators in the United States.

### 2.4. Metabolism

Humans represent the dominant source of metabolic heat in urban areas. So, for the purposes of this study other animals are neglected. To estimate heat release from human metabolism we first note that metabolic rates are not constant over the course of a day. Specifically, using data from (Fanger, 1972; Guyton, 1986) the sleeping metabolic rate for a typical 70kg man is about 75 W. During the daytime this metabolic rate increases depending upon the activity. For the purposes of this study we assume that daytime metabolic rates in urban areas on average are 175 W transitioning to 75 W at night. For most cities this is a relatively small component of the total heating profile (< 10%). Since it is easily incorporated, however, we include it here.

### 2.5 $Q_f$ Profiles for Philadelphia

The process outlined above has been applied to Philadelphia, generating a nominal summer and winter profile for anthropogenic heating. These profiles are for the city as a whole, and it should be noted that the actual magnitude of $Q_f$ within the urban core is likely to be substantially higher than the values given in Figure 3. Likewise, the profile magnitudes in residential areas are likely to be lower. Nevertheless, the profiles developed for the city as a whole offer a useful approximation that can be used in mesoscale modeling of the city in an attempt to identify the potential role of $Q_f$ in the formation of the UHI.

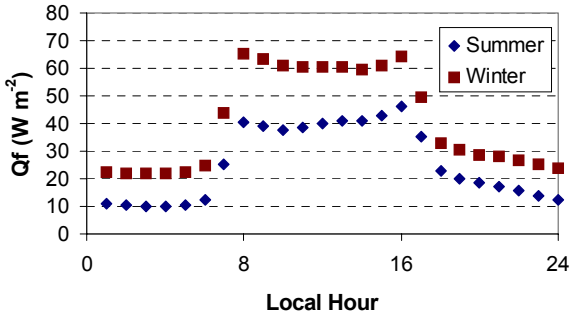


**Figure 3**. Diurnal profiles of anthropogenic heating for Philadelphia in summer and winter.

## 3. INCORPORATING QF INTO THE MM5

Waste heat released in the urban environment can initially enter the substrate or can be emitted directly into the near-surface air. For example, heat released due to air conditioning of buildings is vented directly into the atmosphere. This is also the case for heat released from tailpipe emissions of vehicles. On the other hand, the heat associated with building energy consumption in winter is not vented through air conditioning and makes its way to the air in the urban canopy through conduction/convection processes in building walls and via normal leakage (air exchanges). These processes introduce a lag in the response of the urban atmosphere to building energy consumption. While atmospheric models do not explicitly include building interiors, this lag is conceptually consistent with putting anthropogenic heat into the surface/substrate of an atmospheric model. Hence, it is useful to implement anthropogenic heating in atmospheric models in such a way that we can explore variations in how this heat is partitioned between the air and substrate. The exact distribution is difficult to specify, but as a starting point it is useful to compare the two extreme cases where all $Q_f$ is put into (a) the near-surface air and then (b) the substrate.

There are various ways in which $Q_f$ can be added into the mesoscale model. We chose to implement it at each time step during the call to the boundary-layer scheme. As the model being used (MM5) allows for multiple choices of boundary-layer schemes, we chose to investigate how $Q_f$ impacts model performance under two separate PBL schemes – Blackadar (BL) and Gayno-Seaman (GS).

Under stable atmospheric conditions the Blackadar scheme uses a local mixing approach (K-theory) to calculate the vertical eddy fluxes of heat, moisture and momentum. In this approach, the fluxes are determined by local gradients. Under the free-convection condition (unstable), the BL scheme employs a non-local mixing approach in which buoyant plumes from the surface mix directly with all other layers in the PBL. The vertical mixing is not determined by local gradients, but by the thermal structure of the whole mixed layer. In such a case, the vertical mixing can be visualized as taking place between the surface layer and each atmospheric layer in the PBL. The vertical turbulent mixing in the unstable situation is much stronger than that in the stable case due to large-eddy turbulent motion. Figure 4 illustrates the local and non-local mixing of turbulent fluxes.

Unlike the Blackadar scheme which uses first-order closure, the Gayno-Seaman (G-S) scheme employs a hybrid approach. Specifically, G-S uses a second-order equation to predict TKE, and first-order closure to calculate other turbulent fluxes, making it a "1.5-order" method. The turbulent heat flux in G-S is given by

$$\overline{w'\theta_l'} = -K_h\left(\frac{\partial \theta_l}{\partial z} - \gamma_g\right) \quad 0 < z < h \qquad (4)$$

Where, $\theta_l$ is the liquid potential temperature and h is the PBL height.

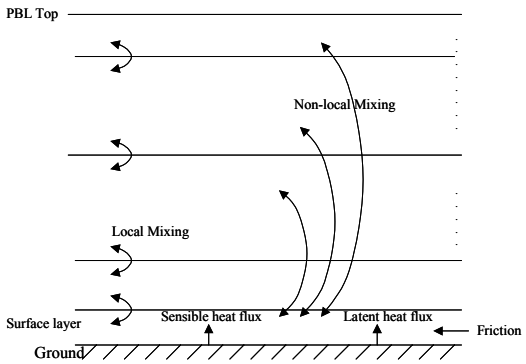


**Figure 4**. Local and non-local mixing of turbulent fluxes

The G-S approach is like a local mixing form, but comparing with K-theory the equation includes an extra term $\gamma_g$, referred to as a counter-gradient heat flux. Its value is related to surface sensible heat flux. This counter-gradient heat flux can be interpreted as a non-local flux of $\theta_l$. Its existence represents the boundary-layer filling convective eddies transporting the surface heat flux upward regardless of the local gradient of $\theta_l$. In G-S $\gamma_g$ is only considered under convective conditions.

The morning boundary-layer transition occurs right after sunrise. During that period PBL stability transits from a nocturnal stable condition to a daytime convective condition. G-S deals with the turbulent heat mixing during the morning transition by considering the counter-gradient heat flux term $\gamma_g$. But the Blackadar scheme calculates the turbulent fluxes in the morning transition uses the local mixing approach. As a result the Blackadar method may underestimate the intensity of turbulent mixing between the surface layer and the other PBL layers. This may cause less upward transport of heat from the surface layer at the time that solar heating of the surface becomes strong. We have found that this mechanism can produce discontinuities in the near-surface air temperature. To improve the performance of the Blackadar scheme during the morning transition, we have modified it to use the non-local mixing approach to calculate the turbulent fluxes during this transition period. This modification has virtually no impact on the boundary-layer dynamics except to remove the morning "jump" in the temperature profile.

## 4. PHILADELPHIA AS A CASE STUDY

While we have developed $Q_f$ profiles for a number of cities (Sailor et al., 2003) our initial testing with the MM5 has focused on two cities. Implementation in simulations of Atlanta showed relatively little impact, in large part due to the modest magnitude of $Q_f$ (about 15 W $m^2$). The simulations for Philadelphia have proven to be more interesting and are the focus of the present work.

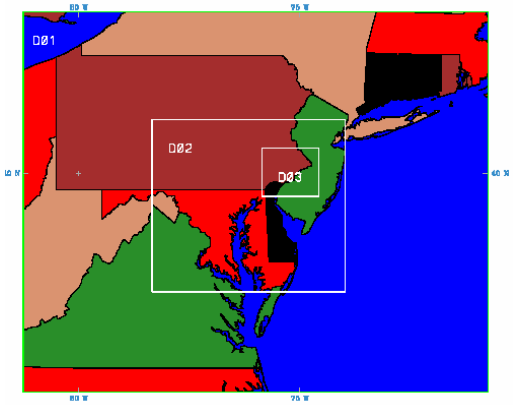


**Figure 5**. Nested modeling domains for Philadelphia. Grid cell resolutions are 18, 6, and 2km.

The Philadelphia domain consists of three nest levels with resolutions of 18, 6, and 2km (Figure 5). The innermost domain was centered on Philadelphia. As the focus is on testing the role of anthropogenic heating in urban mesoscale modeling we have implemented a relatively bare-bones version of the MM5 v3.4. No urban canopy parameterization is used, and land use patterns were modified only slightly from the default USGS land use data to more accurately represent the current extent of the urban development.

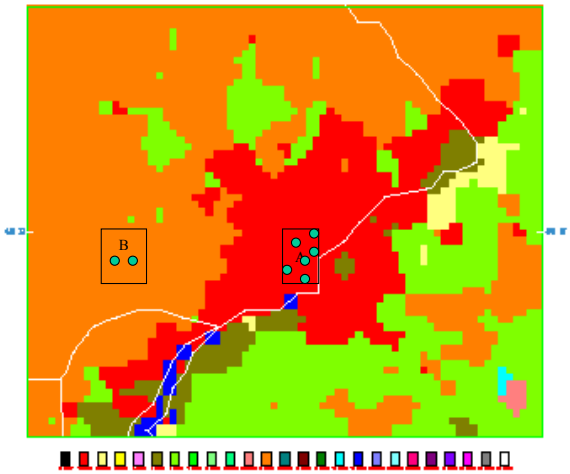


**Figure 6**. Land use in the urban domain (red is urban). The boxes denoted by "A" and "B" represent the urban core and representative rural regions respectively.

Observational data for Philadelphia were available from the Automated Weather Source AirWatch network of weather stations located at local schools. These stations use standardized meteorological equipment and siting requirements. In Philadelphia there are roughly 40 such sites located across the metropolitan area and in the suburbs. We define two control areas in Figure 6. Area "A" is in an urban setting in the central portion of the city and contains 6 of the AirWatch schools. Area "B" is a suburban location where 2 of the AirWatch schools are located. In discussing meteorological characteristics of either area we use an average of the corresponding AirWatch stations to represent observed values and the modeled values are obtained from an average of the MM5 surface air layer grid cells within these boxed areas.

We identified representative summer and winter periods to simulate. For each season two series of model runs were performed (1) using the Blackadar boundary-layer scheme and (2) using the Gayno-Seaman (G-S) boundary-layer scheme. Each series of model runs consists of a base case and cases where the profiles of Figure 3 were input either into the surface air layer or entirely into the ground surface energy budget.

### *4.1 Summertime simulations*

The summertime simulations were for UTC 0:00 8/10/2002 – 0:00 8/12/2002. This was a period of relatively clear sky conditions, somewhat representative of a typical summer day.

For the summer simulations the G-S scheme performed better than the Blackadar scheme although both underestimated daytime temperatures by about 1 and 3 $^oC$ respectively. The nocturnal cooling rates of the two implementations were comparable to the observed cooling rates, and so the nocturnal temperatures predicted by the models were also less than the

observed temperatures (although there was some convergence of observations and model prediction).

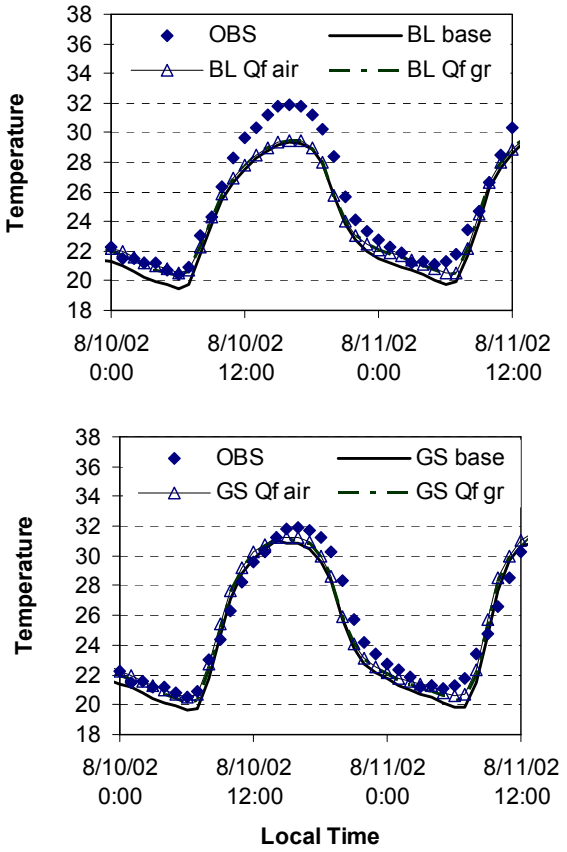


**Figure 7**. Near-surface urban (area A) air temperatures for the summer simulation.

In summer the anthropogenic heating profile ranges from about 10 W $m^2$ at night to around 40 W $m^2$ during the day. This compares with typical peak daytime insolation levels around 850 W $m^2$. The result is a relatively small increase in air temperatures associated with including anthropogenic heating in either the air or ground surface layers.

### *4.2 Wintertime simulations*

The simulation period for winter was chosen to be UTC 0:00 2/23/2002 – 0:00 2/25/2002. As with the summer date, this too was a relatively calm, clear, and somewhat typical winter day.

In winter the anthropogenic heating profile ranges from about 20 W $m^2$ at night to around 60 W $m^2$ during the day. Thus, the nocturnal anthropogenic heating in winter is about double that in summer. The daytime anthropogenic heating is also substantially larger than that for summer (about 1.5 times). At the same time, the peak daytime insolation levels in winter are typically in the range of 400 W $m^2$ (about half of the summer magnitude). These factors set the stage for anthropogenic heating being of much more consequence in the winter simulations. As shown in Figure 8 the result is a notable increase in air temperatures associated with including anthropogenic heating in either the air or ground surface layers. This is the case for both the Blackadar and Gayno-Seaman simulation results.

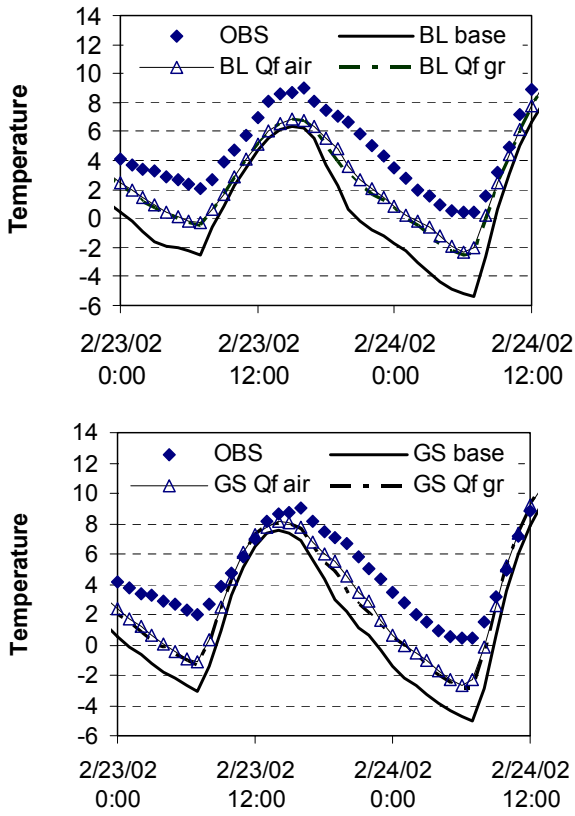


**Figure 8.** Same as figure 7, but for the winter simulations.

As is evident in Figure 8 both implementations of the model were again cooler than observations. In contrast to the summer simulations, however, the nocturnal modeled and observed temperature profiles diverged. Thus, the model runs indicate significantly more cooling at night than is actually occurring in the urban area. Part of this cooling is likely explained by a reduced sky view factor for long wave radiative cooling and other complexities of the urban canopy neglected in the present implementation of the MM5, that may be accounted for in an urbanized version of the model (e.g., Lacser and Otte, 2000). Nevertheless, we argue that a portion of this difference is due to the lack of representation of anthropogenic heat release in the baseline mesoscale model. This argument is supported by the clear impact that anthropogenic heat has on the nocturnal temperature profile. As illustrated in Figure 9 the nocturnal impact of anthropogenic heating is 2 and 3 $^oC$ for the G-S and BL implementations, respectively. This represents about half of the difference between the

baseline simulations and observations. The interesting feature shown in this figure is how addition of $Q_f$ into the ground heat budget impacts air temperatures relative to its inclusion in the near-surface air. Specifically, when $Q_f$ is added into the ground it has nearly the same (small) impact during the day, and only slightly less impact at night.

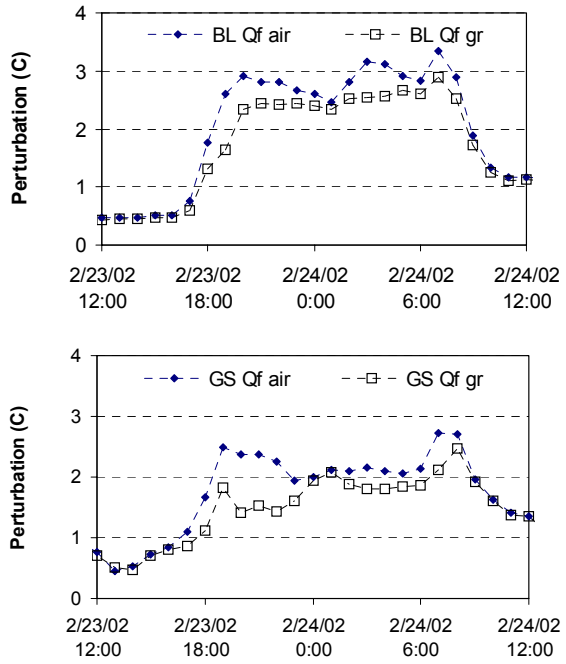


**Figure 9**. Temperature elevations caused by addition of anthropogenic heating in the winter simulations.

Another way of investigating the impact that inclusion of anthropogenic heating has on meteorological simulations of the urban environment is to compare observed heat island signatures with those computed by the atmospheric model with and without anthropogenic heating. By looking at temperature differences we remove some of the systematic bias of the MM5 simulations, and can focus more on the relative impact of anthropogenic heating. The observed heat island is calculated based on the difference between the average temperatures within areas "A" and "B" at any hour during the simulation periods. The modeled heat island is based on averages of near-surface air temperature over the grid cells within these defined areas. The winter UHI magnitudes are compared in Figure 10 for both implementations of the model (G-S and BL). The observed UHI is about 2 $^{o}$C during the day and about 3 $^{o}$C at night. The daytime value of the UHI is captured relatively well by both the baseline BL and G-S PBL implementations, but is underestimated by about 3 to 4 $^{o}$C at night (both schemes give a negative UHI at night, ie., a "cool island"). The inclusion of anthropogenic heating has little impact on the modeled UHI during the day, but reduces the nighttime UHI errors by 2 to 2.5 $^{o}$C. This result suggests that anthropogenic heating may be relatively unimportant in the development of the daytime UHI but dominates the nighttime UHI effect.

## 5. CONCLUSIONS

Anthropogenic heat release in urban environments has distinct diurnal and seasonal characteristics. In Philadelphia the nighttime value of anthropogenic heating is roughly 10 and 20 W m$^2$ for summer and winter seasons. The corresponding daytime values are about 40 and 60 W m$^2$. When these profiles are implemented in an atmospheric model of the urban area the resulting impact on near-surface air temperatures appears to be more sensitive to boundary-layer parameterization scheme than to the method of heat addition (into air vs. soil).

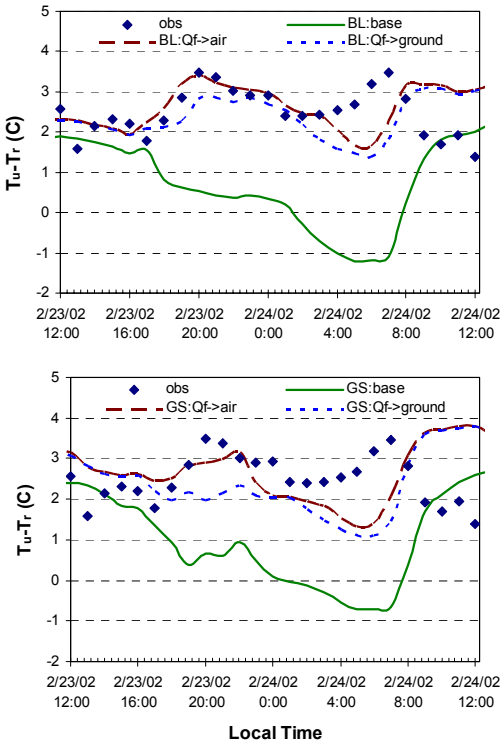


**Figure 10**. Observed and modeled urban heat island intensities for the winter simulations.

A basic implementation of the mesoscale model for a winter simulation of Philadelphia (using the Gayno-Seaman PBL scheme) underestimates daytime temperatures by about 1 to 1.5 $^{o}$C, but underestimates nighttime temperatures by as much as 5 $^{o}$C. Inclusion of anthropogenic heating in this simulation (either in the air layer or ground surface) reduces these errors by about 0.5 and 2 $^{o}$C during the day and night respectively. Although there are numerous other causes for the errors in this winter simulation, the results suggest that about 30-50% of the error may be due to the original model not accounting for anthropogenic heating.

A similar story is evident in analysis of the observed and modeled wintertime UHI effect. Anthropogenic heating has little impact on the modeled UHI during the day, but reduces the nighttime UHI errors by more than 50%.

Ongoing simulations in which $Q_f$ is added to the subsurface soil layers are intended to better represent the time lag associated with heat storage in buildings. Finally, the reader should be cautioned that broad generalizations should not be made from such a limited suite of simulations. Nevertheless, these results do suggest the potential importance of anthropogenic heating, particularly during night and winter. It is also likely, however, that anthropogenic heating in urban environments has an important role in transitional boundary-layer dynamics in the early morning hours, and may therefore be of particular importance with respect to atmospheric mixing and dispersion processes. Higher spatial resolution of anthropogenic heating profiles may also help to improve our ability to capture the UHI in mesoscale modeling simulations.

**Acknowledgments.** Mr. L. Lu was instrumental in developing the anthropogenic heating profiles used in this work. This work was funded in part by NASA through the Louisiana Board of Regents DART program, under Contract No. NASA/LEQSF(2002-03)-DART-03.

## 6. REFERENCES

Carlson, T. N.Arthur, S. T., 2000. The impact of land use - Land cover changes due to urbanization on surface microclimate and hydrology: A satellite perspective. *Global and Planetary Change*, **25,** 49-65.

Dreher, D. B.Harley, R. A., 1998. A Fuel-Based Inventory for Heavy-Duty Diesel Truck Emissions. *Journal of the Air & Waste Management Association*, **48,** 352-358.

Fanger, P. O., 1972. Thermal Comfort: Analysis and Applications in Environmental Engineering. McGraw-Hill, 244 pp.

Fujino, T., Asaeda, T., Wake, A., 1996. Numerical experiment on the characteristics of temperature distribution in metropolitan areas in summer. *Geographical Review of Japan, Series A*, **69A,** 817-831.

Fulton, P. N., 1984. Estimating the Daytime Population with the Urban Transportation Planning Package. *Transportation Research Record*, **981,** 25-27.

Gammariello, R.Carlock, M., 1997: Development of hourly vehicle activity for estimating vehicle emissions. *Seventh CRC On-Road Vehicle Emission Workshop*, San Diego, CA, California Air Resources Board (www.arb.ca.gov), 1001 "I" Street, P.O. Box 2815, Sacramento, CA 95812, 16.

Guyton, A. C., 1986. Textbook of Medical Physiology. W.B. Saunders Company, 1057 pp.

Hafner, J.Kidder, S. Q., 1999. Urban heat island modeling in conjunction with satellite-derived surface/soil parameters. *Journal of Applied Meteorology*, **38,** 448-465.

Hallenbeck, M., Rice, M., Smith, B., Cornell-Martinez, C., Wilkinson, J., 1997: Vehicle Volume Distribution by Classification. Washington State Transportation Center (http://depts.washington.edu/trac), University of Washington, 1107 NE 45th St. Suite 535, Seattle WA 98105, 54 pp.

Ichinose, T., 1999. Impact of anthropogenic heat on urban climate in Tokyo. *Atmospheric Environment*, **33,** 3897-3909.

ISTHA, 1998: Market Analysis Northwest Corridor Transit Feasibility Study. Illinois State Toll Highway Authority.

Lacser, A.Otte, T. L., 2000: Implementation of an Urban Canopy Parameterization in MM5. *Preprints, Forth Symposium on the Urban Environment*, Norfolk, VA, AMS, 153-154.

Larsen, L. C., 2000: Freeway Traffic and Air Quality in the South Coast Air Basin: Diurnal Patterns by Day of Week. California Air Resources Board (www.arb.ca.gov), 1001 "I" Street, P.O. Box 2815, Sacramento, CA 95812, 10 pp.

Owen, T. W., Carlson, T. N., Gillies, R. R., 1998. An assessment of satellite remotely-sensed land cover parameters in quantitatively describing the climatic effect of urbanization. *International Journal of Remote Sensing*, **19,** 1663-1681.

Sailor, D., 2003. A top-down methodology for developing diurnal and seasonal anthropogenic heating profiles for urban areas. *submitted, Atmospheric Environment*.

Sailor, D., Lu, L., Fan, H., 2003: Estimating urban anthropogenic heating profiles and their implications for heat island development. *Fifth Int. Conf. Urban Climate*, Lodz, Poland.

Sailor, D. J., Rosen, J. N., Muñoz, J. R., 1998. Natural Gas Consumption and Climate: a Comprehensive Set of Predictive State-Level Models for the United States. *Energy- the international journal*, **23,** 91-103.

Taha, H., Akbari, H., Sailor, D., Ritschard, R., 1991. Heat Island and Oasis Effects of Vegetative Canopies: Micro-Meteorological Field-Measurements. *Theor. Appl. Cimatol*, **44,** 123-138.